THE JOURNAL OF BIOLOGICAL CHEMISTRY
Vol. 276, No. 43, Issue of October 26, pp. 40293–40297, 2001
© 2001 by The American Society for Biochemistry and Molecular Biology, Inc.
Printed in U.S.A.

Mitochondrial [Ca^{2+}] Oscillations Driven by Local High [Ca^{2+}] Domains Generated by Spontaneous Electric Activity*[S]

Received for publication, August 16, 2001, and in revised form, September 4, 2001
Published, JBC Papers in Press, September 10, 2001, DOI 10.1074/jbc.C100465200

Carlos Villalobos, Lucía Núñez, Pablo Chamero, María Teresa Alonso, and Javier García-Sancho‡

From the Instituto de Biología y Genética Molecular (IBGM), Universidad de Valladolid and Consejo Superior de Investigaciones Científicas, Departamento de Fisiología y Bioquímica, Facultad de Medicina, E-47005 Valladolid, Spain

Mitochondria take up calcium during cell activation thus shaping Ca^{2+} signaling and exocytosis. In turn, Ca^{2+} uptake by mitochondria increases respiration and ATP synthesis. Targeted aequorins are excellent Ca^{2+} probes for subcellular analysis, but single-cell imaging has proven difficult. Here we combine virus-based expression of targeted aequorins with photon-counting imaging to resolve dynamics of the cytosolic, mitochondrial, and nuclear Ca^{2+} signals at the single-cell level in anterior pituitary cells. These cells exhibit spontaneous electric activity and cytosolic Ca^{2+} oscillations that are responsible for basal secretion of pituitary hormones and are modulated by hypophysiotrophic factors. Aequorin reported spontaneous [Ca^{2+}] oscillations in all the three compartments, bulk cytosol, nucleus, and mitochondria. Interestingly, a fraction of mitochondria underwent much larger [Ca^{2+}] oscillations, which were driven by local high [Ca^{2+}] domains generated by the spontaneous electric activity. These oscillations were large enough to stimulate respiration, providing the basis for local tune-up of mitochondrial function by the Ca^{2+} signal.

Research on Ca^{2+} signaling is evolving from the global (cellular) to the local (subcellular) environment, where changes of [Ca^{2+}] inside organelles also play a prominent role (1, 2). Mitochondria take up Ca^{2+} during cell activation (3–5) thus shaping Ca^{2+} signaling and exocytosis (4, 6, 7). In turn, the increase of mitochondrial [Ca^{2+}] ($[Ca^{2+}]_M$)[1] activates several mitochondrial dehydrogenases (8) thus providing a coupling mechanism to adjust mitochondrial function to the increased needs of active cells (5). Close junctions between mitochondria and the endoplasmic reticulum (5, 9, 10) or subplasmalemmal high [Ca^{2+}] domains (4, 7, 11) have been proposed to couple local mitochondrial function to the Ca^{2+} signal. In several cell systems stimulation has been reported to increase the mitochondrial NADH (12–14) and the synthesis of ATP (15, 16) and other mitochondrial factors required for stimulus-secretion coupling (17).

Aequorin, a Ca^{2+}-sensitive photoprotein, can be directed to a defined cellular location by adding specific targeting sequences, but single-cell imaging of aequorin bioluminescence is difficult because of the very low light output (18). Here we combine superb selectivity of targeted aequorin, high expression induced by a viral vector (4, 19), and high sensitivity provided by a photon-counting camera (20, 21) to resolve changes of [Ca^{2+}] in different subcellular compartments at the single-cell level.

Anterior pituitary (AP) cells and lines derived from them (*e.g.* GH_3 cells) exhibit spontaneous electric activity, Ca^{2+} action potentials, and oscillations of the cytosolic [Ca^{2+}] ($[Ca^{2+}]_c$) that are responsible for basal AP hormone secretion. Hypophysiotrophic factors regulate secretion by increasing or decreasing this spontaneous activity (22, 23). A similar model may apply to other excitable secretory cells. Here we have monitored [Ca^{2+}] in different subcellular compartments of living AP and GH_3 cells by bioluminescence imaging of targeted aequorins with the aim of defining their role in the spontaneous activity and whether this may be relevant to the physiologic function.

EXPERIMENTAL PROCEDURES

Cell Culture, $[Ca^{2+}]_c$ Measurements, and Expression of Aequorins—Culture of GH_3 pituitary cells and rat AP cells and imaging of $[Ca^{2+}]_c$ with fura-2 were as described previously (24, 25). For calculation of oscillation indexes all the differences (in absolute value) between each value and the following one were added and divided by the total number of measurements during the integration period. This parameter is sensitive to both the amplitude and the frequency of oscillations (24). Mitochondrial aequorin (mitAEQ) and low Ca^{2+} affinity mutated mitochondrial aequorin have been described previously (4). Nuclear and cytosolic aequorin cDNAs were obtained from Molecular Probes and cloned in the pHSVpUC plasmid. Packaging and titration of the pHSVnucAEQ (nuclear) and pHSVcytAEQ (cytosolic) viruses were performed as reported (19). Cells (3×10^3/0.5 ml) were infected with 1–3 $\times$ 10^3 infectious virus particles of a defective herpes simplex virus, type 1 containing the corresponding aequorin gene and cultured for 12–24 h before measurements. Infection efficiency ranged between 22 and 60% (mean ± S.E., 38 ± 4%; 734 cells from 10 experiments).

Imaging of Aequorin Bioluminescence and NAD(P)H Fluorescence—Cells expressing apoaequorins were incubated for 1–2 h at room temperature with 1 μM coelenterazine. Coelenterazine n was used for reconstitution of low Ca^{2+} affinity mutated mitochondrial aequorin to decrease further the Ca^{2+} affinity (26). The standard incubation medium had the following composition (in mM): NaCl, 145; KCl, 5; $CaCl_2$, 1; $MgCl_2$, 1; glucose, 10; Na-HEPES, pH 7.4, 10. Cells were placed into a perfusion chamber thermostatized to 37 °C under a Zeiss Axiovert 100 TV microscope and perfused at 5–10 ml/min with the test solutions, prewarmed at 37 °C. At the end of each experiment cells were permeabilized with 0.1 mM digitonin in 10 mM $CaCl_2$ to release all the residual aequorin counts. Bioluminescence images (20, 21) were taken with a Hamamatsu VIM photon-counting camera handled with an Argus-20 image processor and integrated for 10-s periods. Photons/cells in each image were quantified using Hamamatsu Aquacosmos software. Total

* This work was supported by the Spanish Dirección General de Enseñanza Superior (DGES; Grants PB97-0474, APC1999-011, and 1FD97-1725-C02-02). C. Villalobos and L. Núñez hold postdoctoral fellowships from the Spanish DGES, and P. Chamero holds a predoctoral fellowship from the Basque Government. The costs of publication of this article were defrayed in part by the payment of page charges. This article must therefore be hereby marked "*advertisement*" in accordance with 18 U.S.C. Section 1734 solely to indicate this fact.

[S] The on-line version of this article (available at *http://www.jbc.org*) contains Movie 1 and Movie 2.

‡ To whom correspondence should be addressed: IBGM, Dept. Fisiología, Facultad de Medicina, E-47005 Valladolid, Spain. Tel.: 34-983-423085; Fax: 34-983-423588; E-mail: jgsancho@ibgm.uva.es.

[1] The abbreviations used are: $[Ca^{2+}]_M$, mitochondrial [Ca^{2+}]; $[Ca^{2+}]_c$, cytosolic [Ca^{2+}]; $[Ca^{2+}]_N$, nuclear [Ca^{2+}]; AP, anterior pituitary; TRH, thyrotropin-releasing hormone; mitAEQ, mitochondrial aequorin; cps, counts per second.

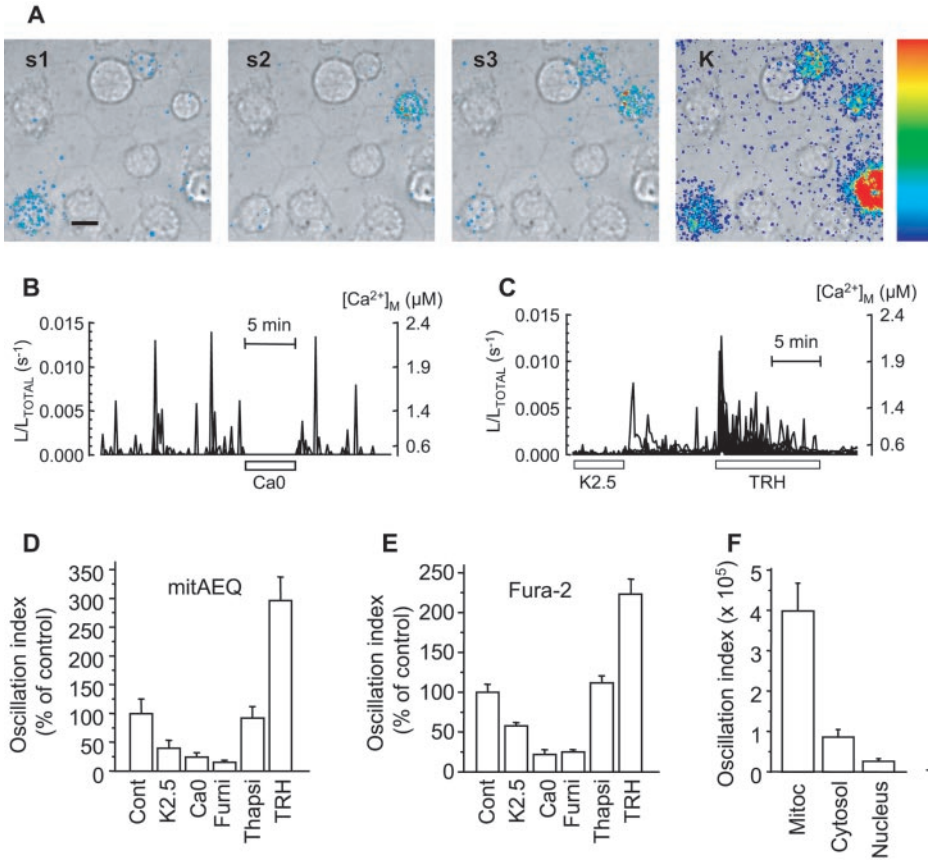

FIG. 1. **Pituitary cells exhibit spontaneous oscillations of mitochondrial [Ca^{2+}].** *A*, luminescence emission of GH_3 cells infected with the mitochondrial aequorin virus (pHSVmitAEQ). The first three images (*s1–s3*) were taken at different times during a 15-min incubation in control medium. *Calibration mark*, 10 μm. Luminescence intensity is coded in pseudocolor (1 to 4 photons/pixel) and superimposed to the gray transmission image taken at the beginning of the experiment. The fourth image (*K*) was taken during a subsequent 10-s stimulation with high K^+ solution (150 mM; replacing the same amount of Na) and coded in pseudocolor (1–40 photons/pixel). Pseudocolor scale is shown at *right*. The integration period was 10 s for all the images. Also available as Movie 1 in Supplemental Material. *B*, effects of extracellular Ca^{2+} removal (*Ca0*; 0.1 mM EGTA added) on spontaneous $[Ca^{2+}]_M$ oscillations of pHSVmitAEQ-infected AP cells. The traces of 6 single cells have been superimposed. *C*, effects of low K^+ (2.5 mM; *K2.5*) and TRH (2 nM) on $[Ca^{2+}]_M$ oscillations of GH_3 cells infected with pHSVmitAEQ. The traces of 15 cells have been superimposed. Also available as Movie 2 in Supplemental Material. *D* and *E*, oscillation indexes (see "Experimental Procedures") of $[Ca^{2+}]_M$, measured with mitAEQ (*D*) and of $[Ca^{2+}]_c$, measured with fura-2 (*E*) in pHSVmitAEQ-infected GH_3 cells. Measurements were performed during incubation with standard medium (*Cont*), low K^+ medium (*K2.5*), Ca^{2+}-free medium (*Ca0*), 1 μM furnidipine (*Furni*), or after stimulation with 2 nM TRH (measured from the 3rd to the 8th min after TRH addition). *Thapsi*, cells pretreated with 0.5 μM thapsigargin for 10 min. Each value is the mean ± S.E. of 23–85 individual cells (two to four experiments). Results are expressed as percent of the controls measured in the same cells. All the values except Thapsi were significantly different from control ($p < 0.001$ to $p < 0.05$, Student's *t* test). In AP cells in primary culture the results were similar. *F*, comparison of the oscillation indexes (see "Experimental Procedures") for the spontaneous oscillations reported by mitochondrial, cytosolic, or nuclear aequorin in GH_3 cells infected with corresponding viruses. Oscillation indexes were computed from the L/L_{TOTAL} (s^{-1}) values. Each value is the mean ± S.E. of 60–272 cells (three to ten experiments). Cytosol and nucleus values were both significantly smaller than the mitochondrial ones ($p < 0.01$).

counts per cell ranged between 2×10^3 and 2×10^5, and noise was (mean ± S.D.) 1 ± 1 cps per typical cell area (2000 pixels). Values refer to the whole cell area. Data were first quantified as rates of photoluminescence emission/total cps remaining at each time and divided by the integration period (L/L_{TOTAL} in s^{-1}, where *L* is luminescence in cps). Emission values of less than 4 cps were not used for calculations. Calibrations in $[Ca^{2+}]$ were performed using the values of the constant published previously (27). A transmission image was also taken at the beginning of each experiment. Oscillation indexes were calculated as described above for fura-2 but using the L/L_{TOTAL} (s^{-1}) values. Mitochondrial NAD(P)H fluorescence (14) was measured using the same set up as for aequorin with excitation at 340 ± 10 nm and emission at 450 ± 40 nm. The integration period was 6 s. For these experiments 1 mM pyruvate was added to the standard medium to keep the cytosolic NAD in the oxidized state.

RESULTS AND DISCUSSION

To investigate whether mitochondrial $[Ca^{2+}]$ oscillations also participate in the spontaneous activity, pituitary cells were infected with a defective herpes simplex virus vector that expresses mitochondria-targeted aequorin (4). Photon-counting imaging of these cells (see Fig. 1*A*, and see Movie 1 in Supplemental Material) revealed clear cut spontaneous $[Ca^{2+}]_M$ oscillations in 40–55% of both GH_3 and AP cells (Fig. 1, *B* and *C*). Depolarization with high K^+ solution evoked a larger $[Ca^{2+}]_M$ increase in the same cells (Fig. 1*A*, *panel K*). To explore whether $[Ca^{2+}]_M$ oscillations could be driven by Ca^{2+} entry secondary to the spontaneous electric activity, we attempted suppression of electrical activity by hyperpolarizing the membrane in low K^+ medium and reducing Ca^{2+} entry by removing external Ca^{2+} or blocking the plasma membrane Ca^{2+} channels with the dihydropyridine antagonist furnidipine. We found that all of these procedures abolished mitochondrial Ca^{2+} oscillations (Fig. 1, *B* and *C*). Fig. 1*D* summarizes the results of several experiments quantified as oscillation indexes, a parameter that is sensitive to both the amplitude and the frequency of the oscillations (see Ref. 24, and see "Experimental Procedures"). Emptying of the intracellular Ca^{2+} stores with thapsigargin did not decrease the $[Ca^{2+}]_M$ oscillations (Fig. 1*D*). Fluorescence imaging of fura-2 revealed spontaneous $[Ca^{2+}]_c$ oscillations, which were also diminished by decreasing

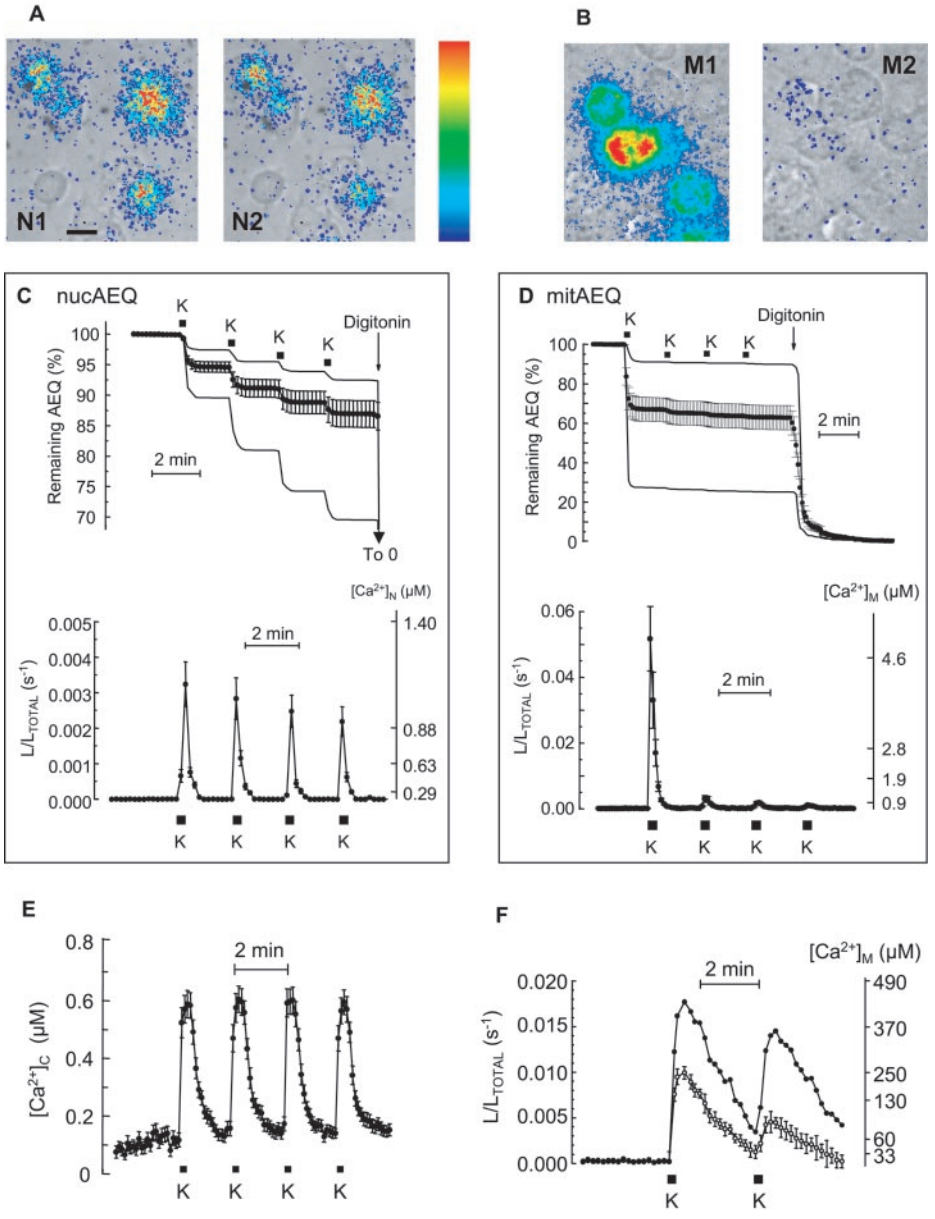

FIG. 2. **Two mitochondrial aequorin pools are revealed by depolarization with high K^+.** Effects of repetitive stimulation with high K^+ on $[Ca^{2+}]_N$, $[Ca^{2+}]_M$, and $[Ca^{2+}]_c$ of GH_3 cells are shown. Cells were stimulated with high K^+ (150 mM, replacing the same amount of Na^+) solution during 15 s every 2 min. *A* and *B*, images taken during the first and second stimulus with high K^+ in cells infected with either the nuclear (*A*) or the mitochondrial (*B*) aequorin virus; other details as in Fig. 1*A*. *C* and *D*, aequorin consumption (*upper trace*) and calibrated signal (*lower trace*) in cells infected with either nuclear (*C*) or mitochondrial aequorin viruses (*D*); *circles* represent the mean of 29 (*C*) and 28 (*D*) single cells; *bars* represent S.E. *Lines* illustrate two single cells with extreme behaviors. The average consumption for the first K^+ stimulus was (mean ± S.E.) 53 ± 6% for the mitochondrial aequorin (10 experiments, 306 cells) and 4.6 ± 0.3% for the nuclear aequorin (3 experiments, 110 cells). *E*, measurements of $[Ca^{2+}]_c$ in pHSVmitAEQ-infected cells loaded with fura-2 (21); mean ± S.E. of 36 single cells. *F*, cells infected with the mutated, low Ca^{2+} affinity, mitochondrial aequorin virus (pHSVmitmutAEQ) and reconstituted with coelenterazine n; *open symbols*, crude data (mean ± S.E. of 20 single cells); *closed symbols*, same data corrected for a pool amounting 50% of the total aequorin counts.

extracellular $[K^+]$, Ca^{2+} removal, and furnidipine, but remained unaffected by emptying the intracellular Ca^{2+} stores (Fig. 1*E*). The hypothalamic releasing factor TRH, which enhances the rate of action potential firing (28), increased both the $[Ca^{2+}]_c$ and the $[Ca^{2+}]_M$ oscillations to similar extents (see Fig. 1, *C–E*; the effect on $[Ca^{2+}]_M$ is also shown in Movie 2 in Supplemental Material). Taken together, these results suggest that the $[Ca^{2+}]_M$ oscillations are generated by the $[Ca^{2+}]_c$ oscillations secondary to the electric activity. To investigate whether this pattern is followed by other subcellular compartments, we imaged cells expressing either the cytosolic or the nuclear aequorin. Both aequorins reported $[Ca^{2+}]$ oscillations that were decreased by Ca^{2+} removal and increased by TRH (not shown), although they were much smaller than the mitochondrial ones (Fig. 1*F*). This suggests the same origin for all the oscillations, but mitochondria are unique in their ability to amplify the Ca^{2+} signal. This organelle can take up large amounts of Ca^{2+} through the mitochondrial Ca^{2+} uniporter at micromolar $[Ca^{2+}]_c$ concentrations (5, 8). Isolated mitochondria can also accumulate efficiently Ca^{2+} through the so-called rapid uptake mode when exposed to trains of Ca^{2+} pulses at concentrations above 0.4 μM (5, 29). In living cells, the rate of uptake is extremely slow at $[Ca^{2+}]_c$ concentrations below 2–4 μM (4, 5). The $[Ca^{2+}]_c$ peaks reported by either fura-2 or cytosolic aequorin were, however, below 0.5 μM. Therefore, the large $[Ca^{2+}]$ oscillations found in mitochondria suggest that local domains with higher $[Ca^{2+}]_c$ are transiently generated nearby.

Aequorin burn-up by Ca^{2+} can be used not only to detect but also to trace the history of high $[Ca^{2+}]$ domains. In populations of chromaffin cells stimulated with brief (10-s) high K^+ stimuli two different mitochondrial pools develop. One takes up very large amounts of Ca^{2+} ($>10^{-4}$ M) whereas the other accumulates a much smaller Ca^{2+} load ($<10^{-5}$ M). Aequorin in the first pool burns out completely during the first high K^+ stimulus and becomes blind to the subsequent stimuli. The different behavior of these two pools is not because of different intrinsic properties but rather because of different spatial locations relative to the plasma membrane Ca^{2+} channels, which determines that they sense local $[Ca^{2+}]_c$ differing by at least one order of magnitude (4). Here we have explored the behavior of pituitary cells, now at the single-cell level. When cells were stimulated with repetitive high K^+ pulses, nuclear aequorin reported a similar light

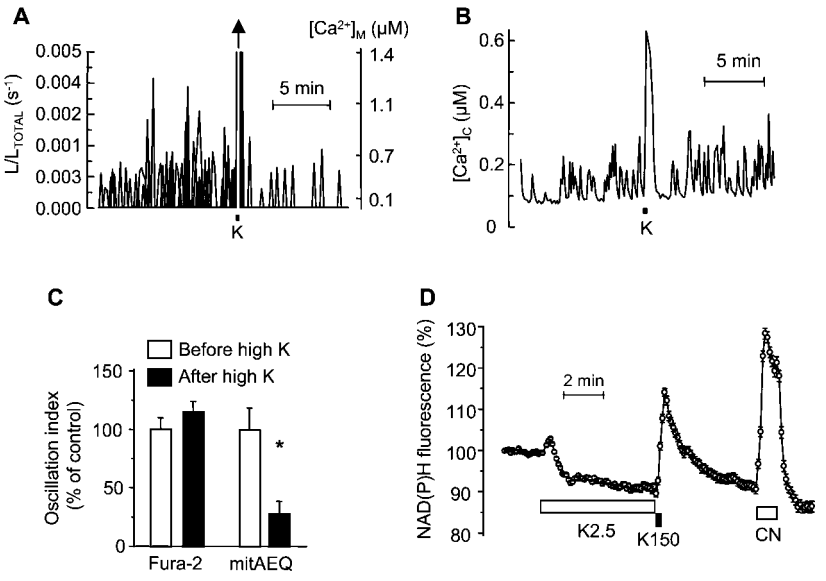

FIG. 3. **Spontaneous $[Ca^{2+}]_M$ oscillations take place in the M1 pool and regulate respiration.** *A*, stimulation with high K^+ (15 s) inhibits subsequent spontaneous oscillations of mitochondrial aequorin luminescence. (GH_3 cells infected with pHSVmitAEQ; traces from seven cells have been superimposed). *B*, the $[Ca^{2+}]_c$ oscillations are not inhibited after stimulation with high K^+ (same cells as in *A* loaded with fura-2; a representative single cell). *C*, mean ± S.E. of the oscillation indexes (see "Experimental Procedures") of 23–72 cells (two to three different experiments). *, $p < 0.001$ (Student's *t* test). *D*, effects of low K^+ (2.5 mM), high K^+ (150 mM), and sodium cyanide (*CN*; 1 mM) on mitochondrial NAD(P)H fluorescence. All values expressed as percent of the initial fluorescence. Each data point is the mean ± S.E. of 61 cells. Blocking cytochrome oxidase with CN promotes maximal NAD(P)H accumulation. In five similar experiments, the decrease of fluorescence by incubation in low K^+ medium was (mean ± S.E.) 6 ± 1%.

output for each stimulus (Fig. 2*A*), but mitochondrial aequorin responded much more strongly to the first stimulus (Fig. 2*B*). In the nucleus each stimulus produced a comparable aequorin consumption (2–5% in average) corresponding to nuclear $[Ca^{2+}]$ ($[Ca^{2+}]_N$) peaks of about 1 μM (Fig. 2*C*). Cytosolic aequorin or fura-2 also reported reproducible $[Ca^{2+}]_c$ rises on repetitive stimulation (Fig. 2*E*). In mitochondria the first stimulus consumed about 40% of the total aequorin whereas each of the following ones consumed only 1–2%, and the first calibrated Ca^{2+} peak was dramatically higher than the subsequent ones (Fig. 2*D*). Even though there was considerable quantitative variation among cells, the qualitative behavior was similar for all the cells (see extreme examples of single-cell traces in Fig. 2, *C* and *D*). In cells permeabilized with digitonin and exposed to Ca^{2+} buffers all the mitochondrial aequorin pool behaved homogeneously (not shown). We interpret the above results in terms of different spatial location of the two mitochondrial pools in the intact cells. The first pool (M1), probably closer to the plasma membrane, takes up large amounts of Ca^{2+} that burn up all its aequorin and render it blind to subsequent stimuli. The second mitochondrial pool (M2) takes up much smaller amounts of Ca^{2+}, and its aequorin remains sensitive to repeated stimulation. The average sizes of M1 and M2 pools were 53 and 47%, respectively. To confirm that blinding of aequorin in the M1 pool was because of complete burn-up by high $[Ca^{2+}]$, the experiments were repeated with a mutated, low Ca^{2+} affinity aequorin, reconstituted with coelenterazine n, which enables $[Ca^{2+}]$ measurements in the 30–1000 μM range (4, 26, 27). Now each stimulus produced a light output that, once corrected for the M1 pool size, revealed repetitive $[Ca^{2+}]_M$ peaks of about 400 μM (Fig. 2*F*). At this concentration the wild type aequorin would be >90% consumed within 1 s (27). As discussed in detail elsewhere (4), the $[Ca^{2+}]$ sensed by M1 and M2 pools must differ by at least one order of magnitude to explain the differences in the rates of mitochondrial uptake. Therefore, our results indicate that subcellular domains with very different $[Ca^{2+}]_c$ are generated during depolarization of pituitary cells with high K^+ and that they are sensed by different, strategically located, mitochondrial pools. A similar organization has been proposed recently in pancreatic acinar cells (7).

Because of physical constraints, the high $[Ca^{2+}]_c$ domains must lie very close to the plasma membrane Ca^{2+} channels (30). Lack of detection by either fura-2 or cytosolic aequorin also suggests that the high $[Ca^{2+}]_c$ domains occupy a very small fraction of the total cytosolic volume. Then, how could Ca^{2+} invade such a large fraction (53%) of the mitochondrial pool? It has been shown recently that continuity of the intramitochondrial space is much larger than thought previously (9, 31). Therefore Ca^{2+} entering mitochondria near the plasma membrane could diffuse throughout the matrix to invade deeper mitochondria. On the other hand, even a random distribution of mitochondria would result in preferential location near the plasma membrane. Because of spherical shape as much as 50% of the cell volume lies within 1 μm from the plasma membrane in a 10-μm-diameter cell.

Do high $[Ca^{2+}]_c$ domains also build up in unstimulated cells? Can such domains account for the spontaneous $[Ca^{2+}]_M$ oscillations? To answer these questions we studied the effects of blinding the M1 pool with a brief high K^+ pulse on the subsequent oscillations. The high K^+ pulse greatly decreased the oscillations reported by mitochondrial aequorin but not those reported by fura-2 (Fig. 3, *A–C*). This suggests that spontaneous $[Ca^{2+}]_M$ oscillations arise from the M1 pool. The increase of $[Ca^{2+}]_M$ to micromolar levels activates several mitochondrial dehydrogenases (8). Increased activity of mitochondrial dehydrogenases results in increased NADH levels (12–14). We find that hyperpolarization with low K^+ solution, which blocks $[Ca^{2+}]_M$ oscillations (Fig. 1*C*), induced a reproducible decrease of NAD(P)H fluorescence (Fig. 3*C*). Removal of external Ca^{2+} had the same effect (not shown). These results suggest that the $[Ca^{2+}]_M$ oscillations are regulating mitochondrial activity even in the basal state. Depolarization with high K^+ (Fig. 3, *D* and *E*) or stimulation with TRH (not shown) produced a clear increase of NAD(P)H fluorescence.

A picture of a highly structured spatiotemporal organization of Ca^{2+} signals emerges from the above results. Mitochondria contribute to shaping local Ca^{2+} domains (4, 7), but, in turn, the Ca^{2+} signal tunes up local mitochondrial function. A mitochondrial subpopulation closer to the plasma membrane is able to monitor the activity of Ca^{2+} channels, and, by taking up Ca^{2+} from local high $[Ca^{2+}]_c$ domains, to increase $[Ca^{2+}]_M$ to levels high enough to activate mitochondrial function to match local energy needs (5) and perhaps to provide other factors required for the secretory process (17). The remaining mitochondria, the bulk cytosol, and the nucleus also sense $[Ca^{2+}]_c$ oscillations but at a smaller amplitude, perhaps adequate for regulation of other cellular functions.

Acknowledgments—We thank Drs. J. Alvarez, J. Llopis, V. L. Lew, and P. McNaughton for helpful comments and J. Fernández for technical assistance.

REFERENCES

1. Alvarez, J., Montero, M. & Garcia-Sancho, J. (1999) *News Physiol. Sci.* **14,** 161–168
2. Berridge, M. J., Lipp, P. & Bootman, M. D. (2000) *Nat. Rev. Mol. Cell. Biol.* **1,** 11–21
3. Rizzuto, R., Simpson, A. W., Brini, M. & Pozzan, T. (1992) *Nature* **358,** 325–327
4. Montero, M., Alonso, M. T., Carnicero, E., Cuchillo-Ibanez, I., Albillos, A., Garcia, A. G., Garcia-Sancho, J. & Alvarez, J. (2000) *Nat. Cell Biol.* **2,** 57–61
5. Rizzuto, R., Bernardi, P. & Pozzan, T. (2000) *J. Physiol.* **529,** 37–47
6. Kaftan, E. J., Xu, T., Abercrombie, R. F. & Hille, B. (2000) *J. Biol. Chem.* **275,** 25465–25470
7. Park, M. K., Ashby, M. C., Erdemli, G., Petersen, O. H. & Tepikin, A. V. (2001) *EMBO J.* **20,** 1863–1874
8. Gunter, T. E., Gunter, K. K., Sheu, S. S. & Gavin, C. E. (1994) *Am. J. Physiol.* **267,** C313–C339
9. Rizzuto, R., Pinton, P., Carrington, W., Fay, F. S., Fogarty, K. E., Lifshitz, L. M., Tuft, R. A. & Pozzan, T. (1998) *Science* **280,** 1763–1766
10. Hajnoczky, G., Csordas, G., Madesh, M. & Pacher, P. (2000) *J. Physiol* **529,** 69–81
11. Kennedy, H. J., Pouli, A. E., Ainscow, E. K., Jouaville, L. S., Rizzuto, R. & Rutter, G. A. (1999) *J. Biol. Chem.* **274,** 13281–13291
12. Pralong, W. F., Hunyady, L., Varnai, P., Wollheim, C. B. & Spat, A. (1992) *Proc. Natl. Acad. Sci. U. S. A.* **89,** 132–136
13. Pralong, W. F., Spat, A. & Wollheim, C. B. (1994) *J. Biol. Chem.* **269,** 27310–27314
14. Hajnoczky, G., Robb-Gaspers, L. D., Seitz, M. B. & Thomas, A. P. (1995) *Cell* **82,** 415–424
15. Kennedy, E. D., Rizzuto, R., Theler, J. M., Pralong, W. F., Bastianutto, C., Pozzan, T. & Wollheim, C. B. (1996) *J. Clin. Invest.* **98,** 2524–2538
16. Jouaville, L. S., Pinton, P., Bastianutto, C., Rutter, G. A. & Rizzuto, R. (1999) *Proc. Natl. Acad. Sci. U. S. A.* **96,** 13807–13812
17. Maechler, P. & Wollheim, C. B. (2000) *J. Physiol* **529,** 49–56
18. Chiesa, A., Rapizzi, E., Tosello, V., Pinton, P., De Virgilio, M., Fogarty, E. & Rizzuto, R. (2001) *Biochem. J.* **355,** 1–12
19. Alonso, M. T., Barrero, M. J., Carnicero, E., Montero, M., Garcia-Sancho, J. & Alvarez, J. (1998) *Cell Calcium* **24,** 87–96
20. Frawley, L. S., Faught, W. J., Nicholson, J. & Moomaw, B. (1994) *Endocrinology* **135,** 468–471
21. Rutter, G. A., Burnett, P., Rizzuto, R., Brini, M., Murgia, M., Pozzan, T., Tavare, J. M. & Denton, R. M. (1996) *Proc. Natl. Acad. Sci. U. S. A.* **93,** 5489–5494
22. Schlegel, W., Winiger, B. P., Mollard, P., Vacher, P., Wuarin, F., Zahnd, G. R., Wollheim, C. B. & Dufy, B. (1987) *Nature* **329,** 719–721
23. Mollard, P. & Schlegel, W. (1996) *Trends Endocrinol. Metab.* **7,** 361–365
24. Villalobos, C. & Garcia-Sancho, J. (1996) *Pflugers Arch.* **431,** 371–378
25. Villalobos, C., Nuñez, L. & Garcia-Sancho, J. (1996) *FASEB J.* **10,** 654–660
26. Alonso, M. T., Barrero, M. J., Michelena, P., Carnicero, E., Cuchillo, I., Garcia, A. G., Garcia-Sancho, J., Montero, M. & Alvarez, J. (1999) *J. Cell Biol.* **144,** 241–254
27. Alvarez, J. & Montero. M. (2001) in *Measuring Calcium and Calmodulin Inside and Outside Cells*. (Petersen, O. H., ed), pp. 147–163, Springer, Berlin
28. Winiger, B. P. & Schlegel, W. (1988) *Biochem. J.* **255,** 161–167
29. Sparagna, G. C., Gunter, K. K., Sheu, S.-S. & Gunter, T. E. (1995) *J. Biol. Chem.* **270,** 27510–27515
30. Neher, E. (1998) *Neuron* **20,** 389–399
31. Skulachev, V. P. (2001) *Trends Biochem. Sci.* **26,** 23–29